Biointerface Research in Applied Chemistry
Open-Access Journal (ISSN: 2069-5837)

Article
Volume 13, Issue 1, 2023, 73
https://doi.org/10.33263/BRIAC131.073

Colorimetric Nanosensor for the Determination of Glyphosate Herbicide in Aqueous Solutions

Cinthia Rocha da Silva [1], Lara Chrystina Malta Neri [1], Thaís Adriany de Souza Carvalho [1], Jhonatan Rafael de Oliveira Bianchi [1], Rodrigo Fernando Bianchi [2], Igor José Boggione Santos [1,*]

[1] Federal University of Sao Joao del Rei, Campus Alto Paraopeba, Department of Chemistry, Biotechnology and Bioprocess Engineering, MG 443 km 7, Ouro Branco-MG, Brazil
[2] Federal University Ouro Preto, Campus Morro do Cruzeiro, Physics Department, Ouro Preto-MG, Brazil
* Correspondence: igorboggione@ufsj.edu.br (I.J.B.S.);

Scopus Author ID 26658712500
Received: 19.11.2021; Accepted: 20.12.2021; Published: 6.02.2022

Abstract: Detection of pesticides depends on complex, time-consuming, and costly techniques performed only in some regions of Brazil. Thus, this study aimed to develop a sensitive, portable, easy-to-handle, and fast nanosensor to determine the presence of glyphosate in aqueous solutions. The $Co(OH)_2$ nanostructure was synthesized, and the kinetic study of the interaction with pesticide glyphosate-based was performed. The $Co(OH)_2$ nanostructures had a fast and effective interaction, confirmed by UV-Visible spectroscopy. Through experimental planning, the process for obtaining nanostructures has been optimized, and the nanostructures obtained were in a size range of 434.2 nm with a hexagonal nanoplate structure. The lower limit of color-based glyphosate detection was 0.178 $g{\cdot}L^{-1}$. It was possible to identify the herbicide in the water of the tomato and sugar cane rinse by the change of the watercolor into pink. Although the samples showed low absorbance, the color change was noticeable to the naked eye. Therefore, to synthesize a structure that allows identifying glyphosate in a colorimetric way.

Keywords: nanotechnology; pesticide; cobalt hydroxide; sustainable agriculture.

1. Introduction

The populational growth causes the demand for food to be on a constant rise, requesting higher efficiency in food production and greater uses of chemical agents such as pesticides [1]. These products are considered a public health problem due to the amplitude of their use, the population exposed to them, and the possibility of causing damage to health [2,3].

The glyphosate-based herbicide is among the main pesticides used in global agriculture. The exacerbated and unsupervised use, in addition to the permanence of its chemical residues in water, food, and environment, poses substantial health risks to the farmers and consumers, besides the environmental damage, such as biodiversity alterations, biological imbalance, and human health disorders, since dizziness until neurological symptoms and death risk, besides that the government and community concern with the half-life period in different conditions [4–6].

The detection of pesticides still depends on qualified personnel and complex techniques, which are slow, expensive, and even fewer sensitive techniques [6], such as chromatography techniques, spectroscopic methods, electrochemical sensors, capillary electrophoresis,

enzyme-linked immunosorbent assays, cell biosensor, cross-responses from multiple sensors [7–9]. Furthermore, it is worth noting that among the existing techniques, none is suitable for performing in-place and real-time tests, which is an urgent demand. These facts place us confronting the challenge of proposing solutions that lead us towards an agricultural practice that integrates three pillars of sustainability: economic, social, and environmental [10,11]. Therefore, it is necessary to search for technologies that allow the determination and identification of pesticides in food, water, and the environment for a conscious and functional use of pesticides.

Advances like these directly imply more effective monitoring of the pollutant levels both in the environment and in food products of human consumption, collaborating to convince government leaders, supervisory authorities, and industries to adopt measures and alternatives compatible with the prospects of sustainability. In this sense, nanotechnology emerges as a promising alternative that allows the development of smaller, more selective, and more sensitive sensors for detecting and monitoring pollutants [12]. There is a need for methods that do not require pre-treatment of samples or pre-or post-derivatization since this is exactly one of the disadvantages of current detection procedures.

The biosensor is potentially used for pesticide detections due to the reaction's selectivity and specificity and has been studied for the past year [7]. However same biomolecules could be expensive and require specific environmental conditions. In this perspective, the fluorescent or the colorimetric sensor using metal nanoparticles are promising devices to detect glyphosate rapidly, helpful for agriculture or government agents. Recently, [13] developed a rapid and fluorescent sensor for carbamate pesticide based on CdTe quantum dots and no zinc 5,10,15,20-tetra(4-pyridil)-21H-23H-porphine, with 5 min of response and LOD compatible with chromatographic techniques.

Nanotechnology, i.e., colloidal metal nanoparticles, are promising materials for sensitive and colorimetric sensors; due to their small size and high surface energy, nanomaterials can decrease the detection limit and increase the selectivity of sensors in addition to generating colorimetric responses not yet known [14,15]. Cobalt hydroxide nanostructures are potential nanomaterials for the colorimetric sensor. Studies show that it is possible to modulate and nanofabricate cobalt; the nanofabricate processing is able to create new proprieties for metal. Is already know some synthesis methods as reduction and surface reconstitutions proposed by Cao and coworkers [16] to create a hybrid nanosheet based on cobalt hydroxide and molybdenum oxide. Also, Onwudine and coworkers [17] synthesized cobalt hydroxide and cobalt oxide nanostructures by green synthesis using extract of *Litchi cinensis* via boiling solutions.

Thereby, this research aimed to develop a sensitive, portable, easy to handle, and fast sensing nanosensor, aiming to determine the presence of glyphosate in aqueous solutions. First, we used the design of the experiment to optimize cobalt hydroxide nano structuration processing to contribute to an easy-way synthesis. Then we present the study of the reaction between glyphosate and nano cobalt hydroxide II to understand kinetic and color changes. Finally, as a proof-of-concept, we tested the colorimetric sensor in the sample from washing tomatoes and sugarcane, which can contribute to achieving sustainable development by monitoring glyphosate pesticide, turning its use more controlled conscientiously.

2. Materials and Methods

2.1. Materials.

Glyphosate-based herbicide original Roundup of the Monsanto industry was used, composed of 445 $g.L^{-1}$ (44.5% $m.V^{-1}$) of N-(phosphonometil) glycine (glyphosate) di-ammonium salt, according to the manufacturer's information. The distilled water was purified in Hidrotek reverse osmosis (Santa Iria de Azóia, Portugal). The other reagents were of analytical grade and were used without further purifications.

2.2. Synthesis of macro and nanostructures of Cobalt Hydroxide II.

Cobalt hydroxide II $Co(OH)_2$ was synthesized via adaptation of the methodology exposed by Heineke and coworkers [18]. The aqueous solution, 0.07 $mol \cdot L^{-1}$, of cobalt chloride hexahydrate ($CoCl_2 \cdot 6H_2O$), was prepared by adding sodium hydroxide (NaOH), 1 $mol \cdot L^{-1}$, until obtaining a pH between 8.0 and 8.5.

Then the solution was centrifuged (Eppendorf Centrifuge 5804/5804 R, BioResearch from Brazil, Germany) for 10 min at 1521 g. The supernatant was discarded, and the pellet was dried in an oven (Bacteriological Greenhouse SL 101/81, Solab, São Paulo, Brazil) at 60 °C for approximately 48 h. The dry solid was macerated and kept stored at 25 °C.

$Co(OH)_2$ nanostructures were produced by dripping the NaOH solution, in the solution of cobalt chloride at 0.07 $mol \cdot L^{-1}$, with the aid of a peristaltic pump (DMC-100, MS Tecnopon Instrumentation, São Paulo, Brazil) for flow control and equipment of heating and magnetic agitation (C-MAG HS 10 IKAMAG) for maintenance of the mixture and temperature control. Then centrifuged (Centrifuge Refrigerated SL 701, Solab, São Paulo, Brazil) the solution at 1521 g for 10 min and subjected the pellet to kiln drying (bacteriological Greenhouse SL 101/81, Solab, São Paulo, Brazil) at 60 °C to constant mass. It was macerated manually with the aid of a pistil and stored at 25 °C.

To identify the optimum conditions for obtaining the nanostructures, the software Statistic 7 was used along with the experimental design of the complete factorial type, which included as an independent variable: temperature and NaOH proportion about to $CoCl_2$ concentration, with the flow of 3 $mL \cdot min^{-1}$, leading to 11 procedures, as shown in Table 1.

Table 1. Experimental design of complete factorial type*.

	Coded variables		Decoded variables	
Assay	**Temperature**	**Proportion NaOH**	**Temperature (°C)**	**Proportion NaOH:$CoCl_2$**
1	-1	-1	40	0.2:1
2	-1	0	40	2.1:1
3	-1	1	40	4:1
4	0	-1	60	0.2:1
5	0	0	60	2.1:1
6	0	1	60	4:1
7	1	-1	80	0.2:1
8	1	0	80	2.1:1
9	1	1	80	4:1
10	0	0	60	2.1:1
11	0	0	60	2.1:1

*Flow: 3 $mL \cdot min^{-1}$.

The experimental design provided the best condition regarding proportion which is 2.1 of NaOH:1 of $CoCl_2$ and 40 or 80 ºC. However, the desired nanostructures size and synthesis conditions have not yet been reached

Therefore, it is necessary to modify some parameters in the procedure for nanostructure synthesis. It was chosen 40 ºC to work because of the low cost and facility. Then it was chosen to work again with flow variation (1, 2, or 3 $mL \cdot min^{-1}$), and alternating the drip distance between the NaOH and $CoCl_2$ solutions (NaOH immerse and emerging in $CoCl_2$). The ultrasonic bath heated to 40 °C and with an ultrasound frequency of 38 kHz (Soniclean 6 Ultrasonic Wash, Sanders Brazil, Minas Gerais, Brazil) was used to dispersion the particles to replace the magnetic stirring plate. According to the previous experimental design, the proportion of 2.1 NaOH:1 $CoCl_2$ was maintained since it provided the best conditions as an optimal region.

Table 2 shows the six procedures performed with a vial containing the cobalt chloride solution positioned inside the ultrasonic bath. After reaching the appropriate temperature for the equipment to operate, the sonification started with the NaOH solution drip.

Table 2. Procedure performed to obtain nanostructure and their variables *.

Assay	Flow ($mL \cdot min^{-1}$)	Drip distance
1	1	immerse
2	1	emerging
3	2	immerse
4	2	emerging
5	3	immerse
6	3	emerging

*Proportion of NaOH : $CoCl_2$ 2,1 : 1.

At the end of the drip, the solution was maintained for a further 5 min, and then taken to centrifuge (Refrigerated Centrifuge Solab SL 701, Solab, São Paulo, Brazil) 812 g for 5 min. After centrifugation, the remaining pellet was subjected to oven drying (SL 101/81 Bacteriological Stove, Solab, São Paulo, Brazil) at 50 °C, for 24 h, followed by manual maceration with the pistil and stored at 25 °C.

2.3. Kinetic of the interaction Glifosato/Cobalt Hydroxide II

The solution of glyphosate was prepared via the addition of 5 mL of the herbicide in 50 mL of distilled water and was added 0.1 g of $Co(OH)_2$ followed by vigorous shaking at 25 °C (Magnetic Agitator DT3120H, DiagTech, São Paulo, Brazil).

At every 5 min, during 45 min and considering the initial time at 0, aliquots were collected from the solution and analyzed in a UV-Visible spectrophotometer (IL-592 Spectrophotometer, IONLAB, Paraná, Brazil) at the wavelength of 525 nm, to identify the absorbance of the complex formed between glyphosate and hydroxide as a function of reaction time.

2.4. Characterization of macro and nanostructures of Cobalt Hydroxide II.

The Fourier-transform Infrared Spectroscopy (FTIR) technique containing Attenuated Total Reflectance (ATR) accessory (Varian 660 Spectrophotometer, PIKE), with a scan of 400 to 4,000 cm^{-1}, was performed at Federal University of Viçosa (UFV, Chemistry Department), to analyze the chemical composition of the synthesized substrates.

Dynamic Light Scattering (DLS) (NanoZetasizer, Malvern England, United Kingdom) from the Multiuser Laboratory of the Pharmacy School (CIPHARMA) at the Federal

University of Ouro Preto (UFOP) was used to analyze the size and the zeta potential of the synthesized structures. This technique allows obtaining the nanostructure hydrodynamic radius and the polydispersity. The equipment consists of an Avalanche Photodiode (APD) detector (Brookhaven, BI-APD, USA) and a correlator (TURBOCORR, Brookhaven, USA) applying a HeNe of 35 mW of power and a wavelength of 632,8 nm as the light source (CVI MellesGriot, USA) linearly polarized. For intensity control, a system of crossed polarizers is used. The samples were analyzed without any filtration.

The thermogravimetric analysis (TGA, Shimadzu DTA-60) and differential scanning calorimetric analysis (DSC, Shimadzu DSC-60 plus) were carried out within N_2 (50 mL·min^{-1}) with a heating rate of 10 ºC min^{-1} in the temperature range 30-600 ºC.

The images of the cobalt hydroxide II nanostructures were obtained by depositing one drop of the sample dispersion on copper grids with Formvar carbon film (Koch Electron Microscopy, Brazil), which was dried at 25°C for 24 h. The images were obtained by the Transmission Electron Microscope (TEM) (Zeiss, 43 model 109, Oberkochen, Germany) with an acceleration voltage of 80 kV. The size of the nanostructures obtained by TEM was performed in the Image J software for all structures larger than 20 nm; in each structure, two measurements were made in the form of x, with a total of 42 structures.

2.5. Influence of glyphosate concentration on the formation of the metallic complex with Cobalt Hydroxide II.

Nine aqueous solution at different concentration of glyphosate were prepared (0.178; 0.356; 0.890; 1.780; 3.560; 7.120; 14.240; 26.700; 53.400 g·L^{-1}). In each solution of 25.0 mL, 0.05 g of $Co(OH)_2$, macro and nanostructured, were added and shaken manually. After 30 min, the dispersions were centrifuged at 4,522 g for 15 min, and the glyphosate concentration was determined in UV-Visible spectrophotometer (IL-592 Spectrophotometer, IONLAB, Paraná, Brazil) at 525 nm.

2.6. Colour analyses.

The color analyses of the system composed of cobalt hydroxide II, macro e nanostructured, were carried out via LAB chromatography (CIELAB - 1976), using Adobe Photoshop CS6 software. The total color difference was calculated as demonstrated in equation 1.

$$\Delta E = \sqrt{L^2 + a^2 + b^2} \quad (1)$$

2.7. Glyphosate identification in tomato and sugarcane.

The 5,6 g·L^{-1} glyphosate solution in distilled water (lethal dose in rats according to Monsanto) was prepared and sprayed on an entire tomato and a piece of sugarcane with bark. They were let rest until they got completely dry to make the glyphosate act. The food was washed with 25 mL of distilled water, reserving the washed water in different flasks. Then 0.05 g of macro- structured $Co(OH)_2$ was added to each sample, which was shaken manually. After 30 min, the dispersions were centrifuged at 4,522 g for 15 min, and the glyphosate presence was determined by UV-Visible spectrophotometer (IL-592 Spectrophotometer, IONLAB, Paraná, Brazil) at 525 nm. The same procedure was performed to identify the glyphosate using the cobalt hydroxide II nanostructured.

2.8. Prototyping.

The sensing device's three-dimensional (3D) model was created in Solidworks software.

2.9. Statistical analyses.

The data obtained in this research were analyzed using the software Excel 2019 for graphical constructions and statistical analysis. Tukey tests ($p < 0.05$) were made unless otherwise.

3. Results and Discussion

3.1. Synthesis and characterization of macro and nanostructures of Cobalt Hydroxide II.

Concerning the cobalt hydroxide nanostructures synthesis, a statistical significance was assessed at the 95% confidence level applying the analysis of variance (ANOVA) in the model of linear interaction versus quadratic interaction to all variables. Table 3 shows the ANOVA data obtained from the complete factorial type design. Figure 1 shows the surface response graph obtained in this design.

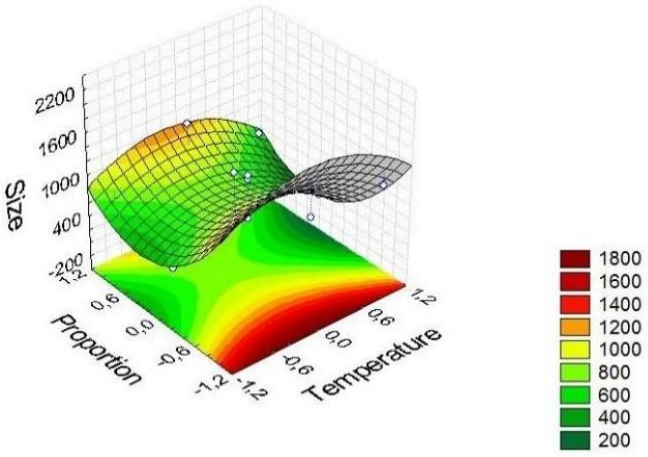

Figure 1. Response surface of the second design of the complete factorial type.

The optimum region is found in the central point worked of proportions (2.1:1 – NaOH:$CoCl_2$), the ideal temperature was 40 ºC or 80 ºC (Figure S3), the chosen on was 40 ºC to reduce energy cost. The smallest size identified with this design was 256.33 ± 103.20 nm, with a polydispersity index of 1.0, suggesting the existence of structures in bigger sizes in the sample that exceed the equipment's identification limit. Statistically significant variables were not identified. However, the F_{tab} value (5.12) was inferior to the F_{calc} value (109.92), confirming the significance of the results as a whole again and not of the isolated variables.

Due to not having found the optimal region by the experimental design, the methodology of $Co(OH)_2$ nanostructures synthesis was altered keeping the proportion and temperature of the experimental design, working with the dispersion by ultrasound, and controlling the drip distance as shown in Table 4 of item 4.4. The ultrasound temperature was kept at 40 ºC. The average size obtained for each treatment and the standard deviation and average polydispersity index (PDI) is shown in Table 4.

Table 3. ANOVA of the data of the second design of the complete factorial type.

Factor	SS	df	MS	F*	P*
Temperature (L)	69245	1	69245.1	0.569179	0.529318
Temperature (Q)	181666	1	181666.3	1.493257	0.346189
Proportion (L)	672921	1	672921.3	5.531265	0.143005
Proportion (Q)	889274	1	889274.4	7.309641	0.113902
Temperature (L)+ Proportion (L)	566437	1	566436.9	4.655987	0.163628
Temperature (L)+ Proportion (Q)	73818	1	73818.3	0.606770	0.517541
Temperature (Q)+ Proportion (L)	589261	1	589261.0	4.843596	0.158718
Temperature (Q)+ Proportion (Q)	122506	1	122506.3	1.006975	0.421312
Error	243315	2	121657.7		
Total SS	3214875	10			

Table 4. Mean size, standard deviation, and polydispersity index of the structures obtained in the different treatments*.

Treatment	Size (nm)	PDI
1	254.9 ± 6.0^{a}	0.395 ± 0.007^{a}
2	$233.4 \pm 28.9^{a,b}$	0.389 ± 0.018^{a}
3	253.6 ± 2.4^{b}	0.498 ± 0.009^{a}
4	209.0 ± 7.0^{a}	$0.392 \pm 0{,}016^{a}$
5	434.2 ± 36.2^{c}	0.668 ± 0.034^{b}
6	255.9 ± 10.1^{a}	0.433 ± 0.062^{a}

*Averages followed by the same letter, in the same column ($p < 0.05$)

The criteria used were the hydrodynamic particle size of a maximum of 300 nm [19] and a PDI value of less than 0.40 [20]. The smallest synthesized structure corresponds to treatment 4. The nanostructures were produced with a flux of 2 $mL \cdot min^{-1}$, with a drip position outside the solution and 40 ºC kept the solution in an ultrasound bath. Therefore, it was decided to use the nanostructures obtained by the methodology of the treatment 4, since even if it did not differ statistically from the other nanostructures, presented smaller size associated with a good PDI, being produced in medium flow, allowing their obtainment in a shorter time when compared to the nanostructures from the treatment 6.

Yang and coworkers [21]synthesized $Co(OH)_2$ nanostructures in the range of 100 to 500 nm by the addition, drop by drop, of 50 mL of NaOH 0.1 $mol \cdot L^{-1}$ into 80 mL of cobalt nitrate ($Co(NO_3)_3$) 0.05 $mol \cdot L^{-1}$ in the sand bath at 45 °C, which was filtered, washed three times with deionized water and dried at 65°C for two days. The authors reported the precipitate formed was pink in color, which differs from the obtained in this research using the cobalt chloride ($CoCl_2$) since the obtained precipitate exhibited coloration in shades of green.

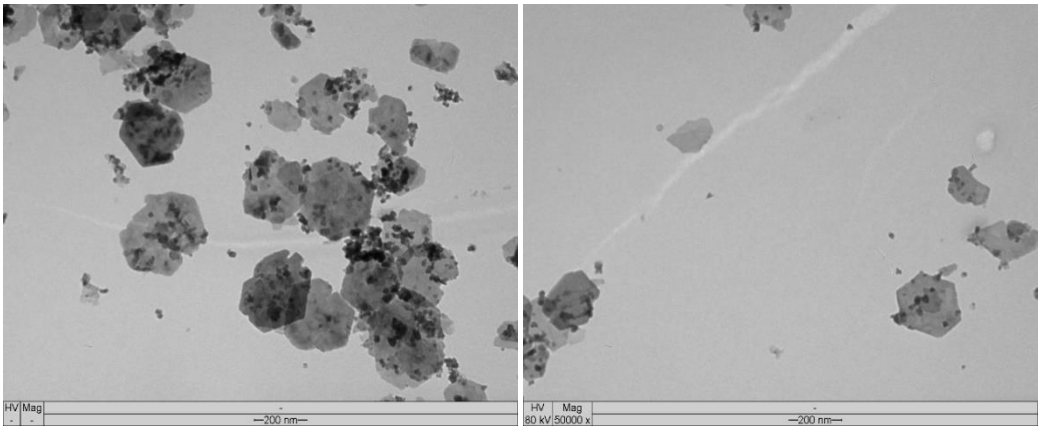

Figure 2. Images via TEM on a scale of 200 nm of nanostructures formed with treatment 4 in different grid regions.

Tian and coworkers [22] synthesized nanobelts dissolving 0.374 g of $Co(NO_3)_2 \cdot 6H_2O$ (3 mol) in 5 mL of distilled water and 1,2-propanediol. The solution was agitated at room temperature for 30 minutes, adding aqueous ammonia. Posteriorly, the solution was autoclaved at 220°C for 24 h. After returning to room temperature, a blue solid formed, filtered, and washed with deionized water and ethanol. The structures showed a thickness and width of 20-50 nm and 200-500 nm, respectively, the width like the one found in this present research of 283.4 nm. Figure 2 shows the images of $Co(OH)_2$ nanostructures obtained at the TEM.

The obtained nanostructures presented the approximate shape predominantly to hexagons, with approximate size to that obtained by DLS (209.0 ± 7.0 nm) and with a tendency to agglomerate.

The average size obtained from the nanostructures on Image J was 207.82 ± 59.14 nm. The polydispersity is shown in the image corroborating with the DLS data. The difference between the sizes obtained by the DLS and the TEM can be justified because the DLS measures the hydrodynamic radius, and the TEM measures the dry structure [23].

Figure 3 shows the obtained green precipitates, and Figure 4 shows the infrared spectrum obtained. Rahbani and coworkers [24] obtained blue color $Co(OH)_2$ by adding NaOH in a gel containing cobalt salt and starch agar. An intense band at 3,628.82 was observed, which can be attributed to free hydrogen, while around 3,400 cm^{-1} is attributed to the hydroxyl groups, which are extensively hydrogen-bonded. The bands identified around 1,600 cm^{-1} may correspond to the mode of deformation of the water molecules vibration; the band at 1,360 cm^{-1} is the CO_2 of air adsorbed in nanostructure [24].

The band around 860 cm^{-1} corresponds to the mode of OH^- deformation [25]. Bands around 400, 500, and 600 cm^{-1} are characteristic of the Co-OH and Co-O stretching vibration, being present in the spectrum specifically at 473.5 and 433.54 cm^{-1} [25–27].

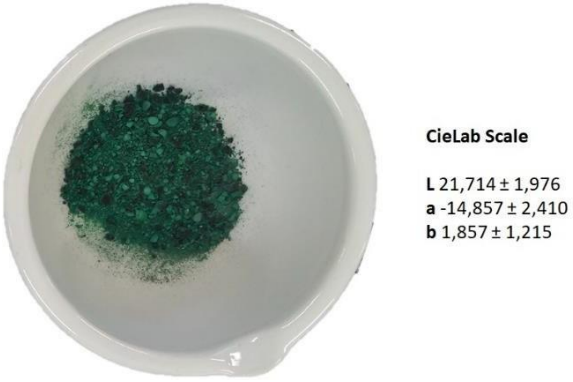

Figure 1. Cobalt Hydroxide II and the CieLab scales.

Li and coworkers [27] obtained $Co(OH)_2$ nanostructures to be applied at pseudocapacitors with bands of the infrared spectrum in 2919, 2850, 1363, 939, 582, 515, and 431 cm^{-1}. The authors attributed the bands around 2900 cm^{-1} as disorders and defects due to the material's amorphous phase, which absorbed H_2O vibrations may have caused. Another study analyzed the FTIR spectrum for $Co(OH)_2$ with 20% of N-methyl pyrrolidone (NMP). Researchers observed characteristic peaks of $Co(OH)_2$ at 3,488; 1,651; 1,695; 1,347; 630 and 523 cm^{-1}
[24,26].

Nanostructures naturally tend to agglomerate for being thermodynamically unstable [28]. Zhu and coworkers [29] showed, in their research, $Co(OH)_2$ nanostructures images

obtained in Field Emission Scanning Electron Microscope (FESEM) and Transmission Electron Microscope (TEM), which also presented hexagonal nanoplate format.

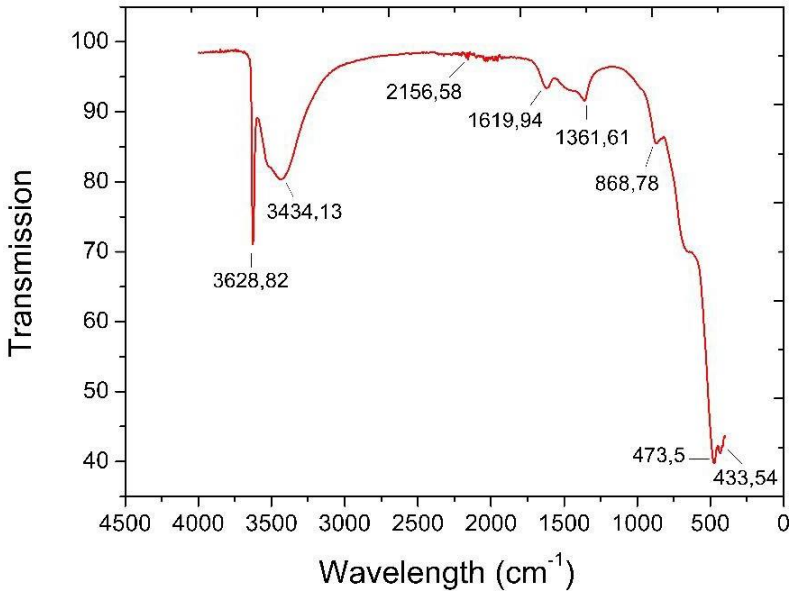

Figure 2. Cobalt Hydroxide II infrared spectrum.

Figure 5 shows a thermal analysis curve of cobalt hydroxide nanoparticles. The gradual loss of mass at temperatures below 150 ºC can be attributed to the evaporation of water adhered to the surfaces of the nanoplates. The dominant mass loss profile exhibits a well-defined decrease over a temperature range of 30-250 °C with two inflection points at about 62.7 and 165.7 °C. The total weight loss was estimated to be 28.37 %, greater than the obtained by Hou and coworkers [30] and Liu and coworkers [31], (3.7 and 17%, respectively. The DSC curve shows an endothermic peak at 100, 185, 250, 400, and 500 °C. The peak at 100 ºC can be assigned to the depletion of surface adsorbed water; the peak at 185 ºC corresponds to the release of interlayer water molecules, and the peaks at 250, 400, and 500 ºC correspond to the collapse of the crystalline structures [32].

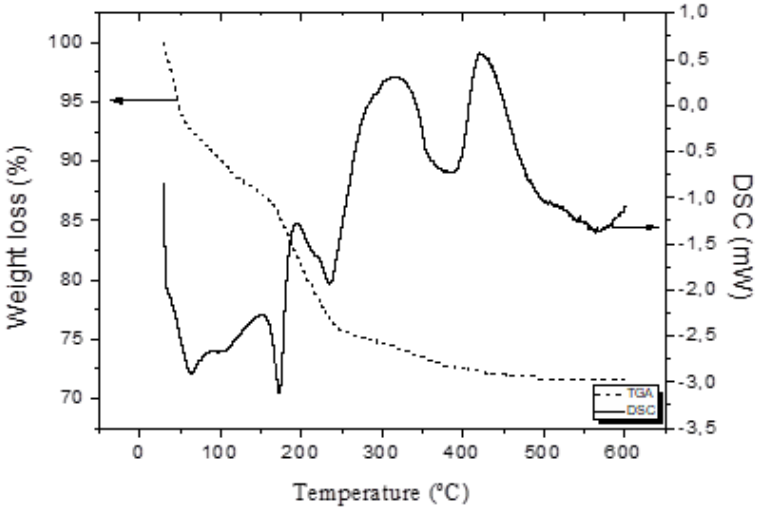

Figure 3. DSC and TGA curves of the $Co(OH)_2$ nanostructures.

3.2. Kinetic test of the reaction between Cobalt Hydroxide and Glyphosate.

Figure 6 shows the detected absorbance as a function of the reaction time after the mixture of cobalt hydroxides II with glyphosate solutions leading to the formation of the metallic

complex glyphosate-cobalt hydroxide (Gly-$Co(OH)_2$). An increase in absorbance was identified along the reaction time due to the higher intensity of the pink color. After 45 min, the reaction of $Co(OH)_2$ with glyphosate solution was completed. Table 5 shows the coefficient of determination of the adjustments of the kinetic models of order zero, first, and second orders to the experimental data.

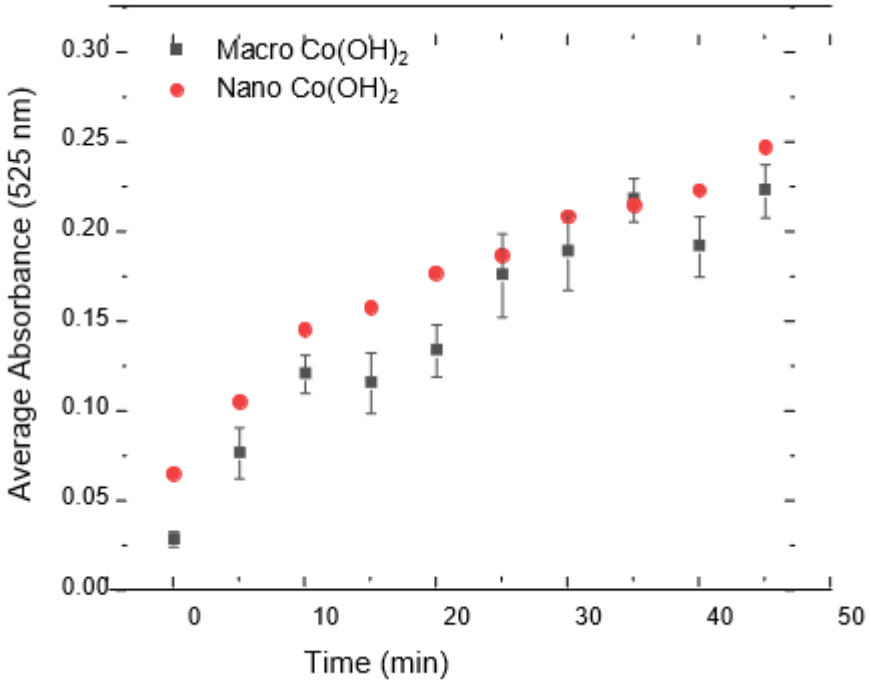

Figure 4. Absorbance data as a function of time for the formation of the Gly-$Co(OH)_2$ metal complex.

Table 5. Coefficient of determination of Co(OH)2.

Substrate	R^2		
	Zero-order	**First-order**	**Second-order**
Macro Co(OH)2	0.8804	0.697	0.4788
Nano Co(OH)2	0.9408	0.8243	0.6665

The Integral Method was utilized to verify the reaction order. The absorbance graph was plotted all-time function - the ratio of the Naperian logarithm of the absorbance and initial absorbance versus the inverse of the absorbance. Then, it was verified that the reaction between the glyphosate solution and Co(OH)2, macro and nanostructured, was zero-order due to the R^2 value, 0.8804 and 0.9408, respectively. In contrast, in the graph of Naperian logarithm and the inverse of absorbance, the value was lower. That fact corresponds to a time constant reaction; that is, the colorimetric alteration occurs at the same time independent of the glyphosate solution concentration, which was confirmed by experimental observation.

Chang and coworkers [33] studied the influence of the time in the catalytic oxidation reaction between 3,3',5,5'-tetramethylbenzidine (TMB), Cu^{2+} and glyphosate, getting a progressive increase in the absorbance along the catalytic reaction time, achieving a maximum absorbance in 20 min, with a slight decrease after that time, this experiment was conducted at 40 °C. However, the methodology is more complex and expensive than the $Co(OH)_2$ nanostrucuration; besides, it can be used at room temperature, facilitating the practical use of the sensor.

In a study for visual detection of glyphosate, Zheng and coworkers [34] utilized gold nanoparticles stabilized in cysteamine (CS-AuNPs) with 30 nm to interact with the glyphosate.

The time and temperature effects on the color change of the reaction were examined. The higher absorbance value was obtained at 15 °C and 8 min. However, with the rising temperature, the shrinkage of the absorbance was observed the time. Besides, the temperature of 15 ºC makes the sensor ineffective as it makes it difficult to use directly on the tillage. Generally, the soil for agriculture must have a temperature between 20 and 30 °C. The shorter time response concerning this work can also be related to the size of the structure, so a reduction in the nano $Co(OH)_2$ this work could improve the sensor response.

3.3. Testing of metal complex formation.

The absorbance test in Uv-Vis was performed to prove the viability of the application of cobalt hydroxide II for the colorimetric determination of glyphosate. Figure 7 shows the average absorbance obtained with solutions containing different volumes of glyphosate with macro and nanostructures of $Co(OH)_2$.

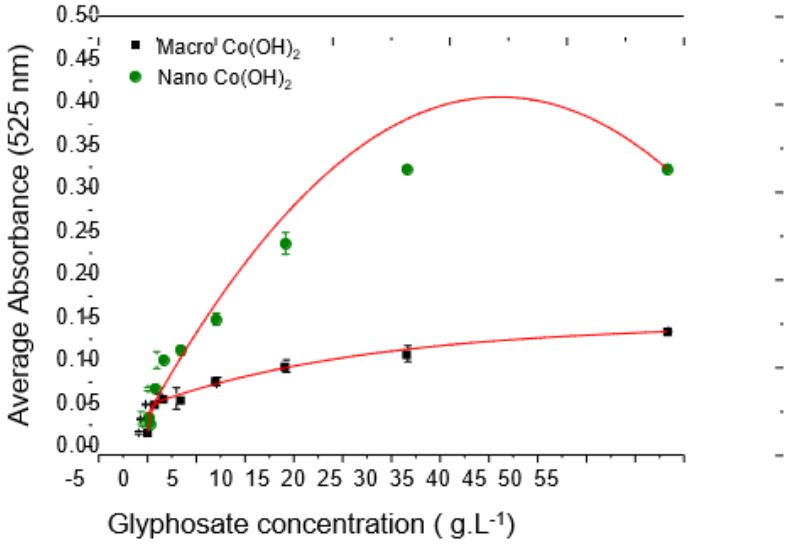

Figure 5. Mean absorbance curve for reactions with $Co(OH)_2$, macro and nanostructured, as a function of glyphosate volumes in 25 mL solution.

The absorbance and color intensity values for all tests were higher in the solutions containing higher volumes of glyphosate, as expected. The nanostructures produced higher absorbance than the macrostructures at the same herbicide concentration. The best fit of the model to the reaction between glyphosate $Co(OH)_2$ macro structured and nanostructured correspond, respectively, to the exponential type 2 (0,999 R^2) and second-order polynomial (R^2 of 0.973). The exponential behavior is explained by the increase in the gradual concentration of glyphosate, maintaining the same mass as $Co(OH)_2$, allowing an increase in the intensity of the color and thus an increase in absorbance. However, by overcoming the stoichiometry of the reaction between glyphosate and $Co(OH)_2$, $Co(OH)_2$ will be the limiting reagent of the reaction, and with that, there will be no more change in color, so after 26.700 $g \cdot L^{-1}$ of glyphosate an absorbance remains the same. Besides, it appears that the absorbance of the pink complex formed between the glyphosate and the nanostructure is greater than with the macrostructure. The results indicate that the $Co(OH)_2$ nanostructures provide a more intense colorimetric response than the macro $Ca(OH)_2$. This advantage of nanotechnology can be explained by the high reactivity of the nanostructure surface. Due to its small size, this increases the area/volume ratio. Therefore, nanotechnology provides high surface energy that increases reactivity [35]. Volumes of glyphosate less than 10 µL (0.178 $g \cdot L^{-1}$) to all analyses did not alter the absorbance

values, 10 µL the detection limit value by UV-Vis spectrophotometry. The optical limit of detection (OLD) was also around that same value. According to the protocol of the Brazilian National Health Surveillance Agency, for non-instrumental methods, the detection limit occurs at the minimum concentration at which the expected effect occurs, in this case, the lowest concentration at which the colorimetric change is observed.

Figure 8A shows the total color difference calculated. It is important to observe the colorimetric change because the initial colorless solution containing a green solid becomes pink, allowing a simple detection of pesticides. By the Tukey test (uppercase) at 10, 20, 50, 100, and 200 µL of glyphosate volume showed a significant difference between nano and macrostructure, also the ΔE for nano $Co(OH)_2$ is higher than macrostructure; therefore, the color change is more perceptible to the human eyes for nano $Co(OH)_2$ than macro $Co(OH)_2$ in the lowest concentration. After 400 µL, the color change is similar. The Tukey test also shows that as the volume of glyphosate increases, the ΔE also increases once all values are statistically different (lower case). Figure 8B shows the optical representation of the colorimetric alteration that occurred in aqueous solutions with different concentrations of glyphosate and $Co(OH)_2$ macro and nanostructured. This sample was also used to calculate the ΔE.

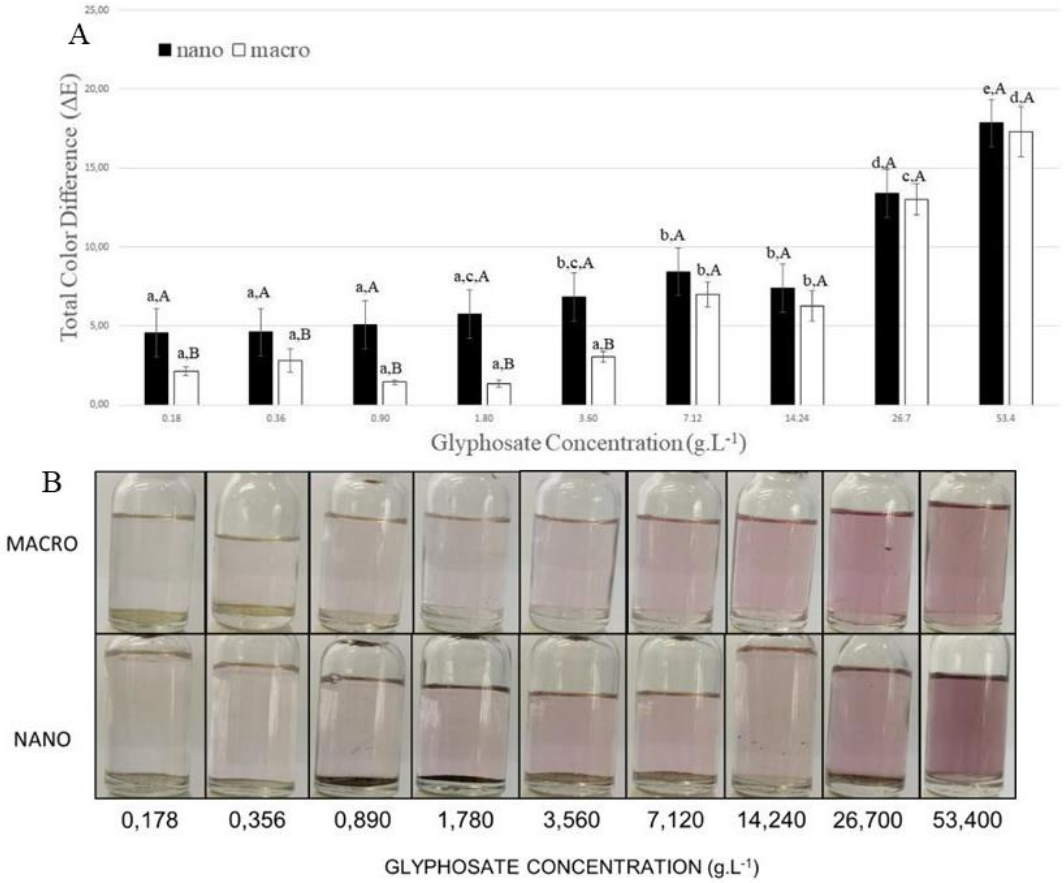

Figure 6. (A) Total Color Difference of the reaction between $Co(OH)_2$ macro and nanostructured and glyphosate in different volumes. Tukey uppercase index represents the analysis between macro and nano at the same volume. Tukey lower case index represents the comparison between the different volumes of each sample. (**B**) Optical representation of the colorimetric alteration occurred in aqueous solutions with different concentrations of glyphosate and $Co(OH)_2$ macro and nanostructured.

Concerning the formation of metallic complexes with glyphosate, there are many studies related to metal complexes between glyphosate and copper, being incipient in the research related to the complexation with other metallic ions [36]. Chang and coworkers [33]

have developed a fluorescence nanosensor for glyphosate, which has decreased fluorescence intensity as glyphosate is added. The nanosensor was synthesized by the combination of copper oxide II (CuO) and MWCNTs and is based on the inhibition of the catalytic activity of CuO/MWCNTs. The detection limit obtained by this method was 6.7 x 10^{-7} g·L^{-1}. However, it presents a subtle color change to the naked eye, from dark pink to light pink, requiring previous sample preparation to be analyzed besides specific equipment for data analyses.

Another method developed for detecting glyphosate is based on the inhibition of the 3,3',5,5'-tetramethylbenzidine (TMB) conversion into oxidized 3,3',5,5'-tetramethylbenzidine (oxTMB) due to the formation of the glyphosate-Cu^{2+} complex, resulting in a change of the solution color. In the absence of glyphosate, the oxidation of TMB to oxTMB catalyzed by Cu^{2+} produces a blue color solution. Still, with glyphosate addition and formation of the glyphosate-Cu^{2+} complex, the blue color fades, and the solution gets a lighter blue color. To perform this methodology, the sample must be at pH 4 and must be heated in a water bath for 20 minutes to a temperature of 40 ºC, making it difficult to apply the method in locu [33].

For the glyphosate determination in water, a colorimetric strip-shaped sensor based on the blue to yellow color change was created from the poly (vinyl) alcohol (cd-PVA) (polyvinyl) doped with copper after injection of the sample of dithiocarbamic acid, which is a compound formed by the derivatization of glyphosate from the reaction of this with carbon disulfide. The limit of detection was 0.1 µg·mL^{-1} and the system sensor was stable for up to 20 days at 23°C. However, the unfavorable point was that interference studies confirmed the susceptibility of this system to compounds and ions found in environmental waters, making pre-treatment of water samples necessary, which takes more time and increases costs, making the technique more complex [37].

3.4. Glyphosate identification in tomato and sugarcane.

Figure 9A shows the average absorbance for the tests of metal complex formation between $Co(OH)_2$ macro-structured and nanostructured ($nCo(OH)_2$) with glyphosate, in solutions prepared in distilled water at 5.6 g·L^{-1} and rinsing water of tomato and sugar cane previously treated with the herbicide. The colorimetric change that can be observed with the naked eye is shown in Figure 9B.

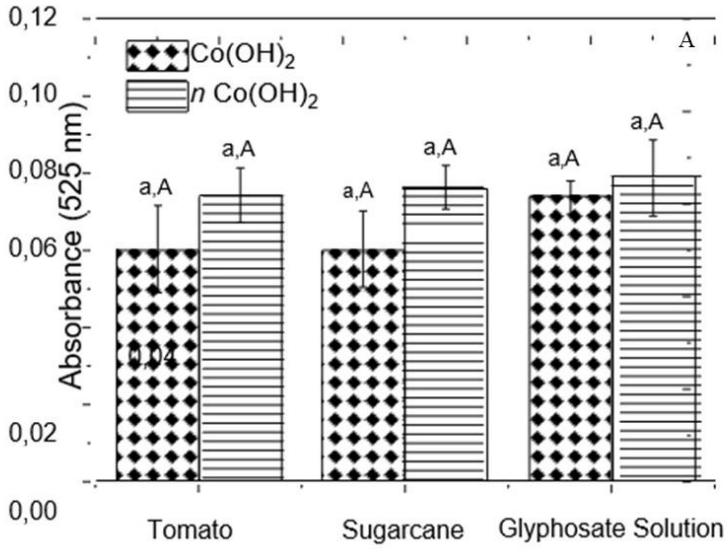

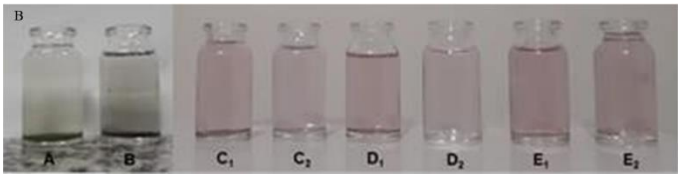

Figure 7. (A) Mean absorbance for tests of metal complex formation between $Co(OH)_2$ and $nCo(OH)_2$ with glyphosate in solutions prepared in distilled water at 5.6 $g.L^{-1}$ and with tomato rinse water and sugarcane. (**B**) Optical representation of the colorimetric alteration occurred in the glyphosate solutions in distilled water and in rinsing water of cane and tomato. A) Distilled water with $Co(OH)_2$; (B) Distilled water with $nCo(OH)_2$; C) Rinsing water from tomato. D) Rising water from sugarcane. E) pure glyphosate.

The values identified for absorbance and color intensity for the three samples tested with $nCo(OH)_2$ were higher than those observed for the $Co(OH)_2$ macrostructure. The glyphosate can be better detected in the solution with distilled water, presenting a lower color intensity in the analyses with rinsing water, either with the macro or nanostructures. Although the 5.6 g.L-1 glyphosate concentration resulted in a low absorbance, it is possible to detect it with the naked eye as expected.

This fact may be related to the adsorption of the herbicide by the food sediments, thus reducing its concentration to the water of rinsing and consequently reducing the number of metallic complexes formed and the coloration exhibited. Besides, the herbicide could be absorbed by food. Moreover, because it's extremely polar, this pesticide is extracted from the aqueous samples and metallic cations and inorganic anions, making it difficult to extract them [18].

3.5. Prototyping.

Figure 10 shows the design of the proposed model and its components. The device prototype was based on a tape model containing immobilized $Co(OH)_2$, presenting a similar operation as a pH evaluation tape. However, the concentration of glyphosate is measured, being a device of easy interpretation and handling. It is seeking the idealization of an unprecedented product with scientific-technological and commercial appeal.

The analyses are based on the immersion of the identifying tape containing the substrate $Co(OH)_2$, which will react with glyphosate in the liquid sample as extract or rinse water. The identification tape should be kept in contact with the sample for at least 30 minutes. After that, the tape may be withdrawn and positioned in the specific compartment for insertion contained in the device. The coloration displayed by the identifying tape can then be compared to the reference color tape, which is positioned in the lower compartment of the device.

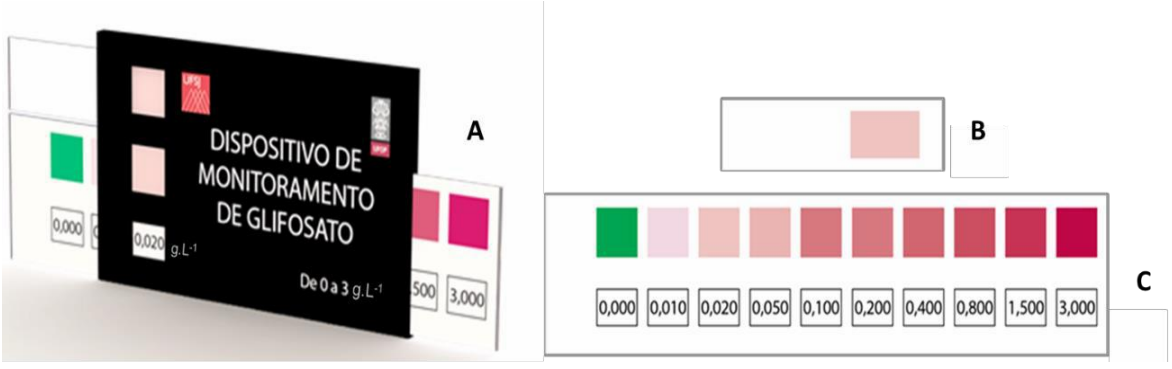

Figure 8. The three-dimensional computational prototype of the sensing device for glyphosate and its components. (**A**) Three-dimensional computational prototype of the sensing device model for glyphosate; (**B**) Identification tape; (**C**) Reference tape for colorimetric comparison.

The reference tape can be moved to both sides until the identification coloration was closest to that expressed by the analyzed sample, thus obtaining the result of the analyses. The advantages of this device are, above all, the ease of handling, the simplicity of interpretation, the possibility of carrying out the *in locu* test in addition to obtaining a short-term response. Lopes and coworkers [38] are based on pH tapes since the device consists of a standard color scale, and a tape dosimeter, a set of colors that are compared to the standard scale, and then the radiation dose applied is identified.

4. Conclusions

$Co(OH)_2$ nanostructures were obtained with a size of 209.0 ± 7.00 nm, polydispersity index of 0.392, and hexagonal morphology. The optical limit of detection of glyphosate using both macro and nanostructured cobalt hydroxide II was 0.178 $g \cdot L^{-1}$. This limit of detection was not altered with the use of $Co(OH)_2$ nanostructures. However, the staining expressed by nanostructures was more intense when compared to the macrostructures.

It was possible to detect glyphosate in tomato and sugarcane rinsing waters. Also, a sensing device model was designed that can become a physical device in the future. Thus, $Co(OH)_2$, both in macro and nanoscale, is an alternative to conventional methods of glyphosate detection due to the colorimetric alteration from its interaction with glyphosate, which allows easy identification of the presence of the herbicide, besides presenting a low response time compared to the analytical methods, allowing the construction of low cost. These portable sensors can be used *in locu*.

Funding

The authors thank the Conselho Nacional de Pesquisa e Desenvolvimento Tecnológico (CNPq), the Coordenação de Aperfeiçoamento de Pessoal de Nível Superior - Brasil (CAPES), and the Fundação de Amparo à Pesquisa do Estado de Minas Gerais (FAPEMIG) the for the financial support.

Acknowledgments

The authors thank CiPharma Multiuser Laboratory of Federal University of Ouro Preto for measures in NanoZeta Sizer, with the project "Asymmetric Flow Field Flow Fractionation" (FAPEMIG CDS – APQ 01510-14) and Núcleo de Microscopia e Microanálise of Universidade Federal de Viçosa.

Conflicts of Interest

The authors declare no conflict of interest.

References

1. Hedlund, J.; Longo, S.B.; York, R. Agriculture, Pesticide Use, and Economic Development: A Global Examination (1990–2014). *Rural Sociology* **2020**, *85*, 519–544, https://doi.org/10.1111/RUSO.12303.
2. Faber, D. Poisoning the World for Profit: Petro-Chemical Capital and the Global Pesticide Crisis. **2020**, *31*, 1–17, https://doi.org/10.1080/10455752.2020.1829794.
3. Paul, K.; Furlong, M.; Yan, Q.; Zhang, K.; Castro, E.; Cockburn, M.; Thompson, L.; Horvath, S.; Bronstein, J.; Ritz, B. Pesticide Exposure, Systems Biology, and Parkinson's Disease. *ISEE Conference Abstracts* **2021**, *2021*, https://doi.org/10.1289/ISEE.2021.O-SY-121.

4. Wang, S.; She, Y.; Hong, S.; Du, X.; Yan, M.; Wang, Y.; Qi, Y.; Wang, M.; Jiang, W.; Wang, J. Dual-Template Imprinted Polymers for Class-Selective Solid-Phase Extraction of Seventeen Triazine Herbicides and Metabolites in Agro-Products. *Journal of Hazardous Materials* **2019**, *367*, 686–693, https://doi.org/10.1016/J.JHAZMAT.2018.12.089.
5. Seralini, G.E.; Jungers, G. Toxic Compounds in Herbicides without Glyphosate. *Food and Chemical Toxicology* **2020**, *146*, 111770, https://doi.org/10.1016/J.FCT.2020.111770.
6. Singh, S.; Kumar, V.; Datta, S.; Wani, A.B.; Dhanjal, D.S.; Romero, R.; Singh, J. Glyphosate Uptake, Translocation, Resistance Emergence in Crops, Analytical Monitoring, Toxicity and Degradation: A Review. *Environmental Chemistry Letters 2020 18:3* **2020**, *18*, 663– 702, https://doi.org/10.1007/S10311-020-00969-Z.
7. Congur, G. An Up-to-Date Review about (Bio)Sensor Systems Developed for Detection of Glyphosate. **2021**, https://doi.org/10.1080/03067319.2021.1950149.
8. Christopher, F.C.; Kumar, P.S.; Christopher, F.J.; Joshiba, G.J.; Madhesh, P. Recent Advancements in Rapid Analysis of Pesticides Using Nano Biosensors: A Present and Future Perspective. *Journal of Cleaner Production* **2020**, *269*, 122356, https://doi.org/10.1016/J.JCLEPRO.2020.122356.
9. Kergaravat, S. v.; Fabiano, S.N.; Soutullo, A.R.; Hernández, S.R. Comparison of the Performance Analytical of Two Glyphosate Electrochemical Screening Methods Based on Peroxidase Enzyme Inhibition. *Microchemical Journal* **2021**, *160*, 105654, https://doi.org/10.1016/J.MICROC.2020.105654.
10. Clapp, J. Explaining Growing Glyphosate Use: The Political Economy of Herbicide- Dependent Agriculture. *Global Environmental Change* **2021**, *67*, 102239, https://doi.org/10.1016/J.GLOENVCHA.2021.102239.
11. Cerdà, A.; Daliakopoulos, I.N.; Terol, E.; Novara, A.; Fatahi, Y.; Moradi, E.; Salvati, L.; Pulido, M. Long-Term Monitoring of Soil Bulk Density and Erosion Rates in Two Prunus Persica (L) Plantations under Flood Irrigation and Glyphosate Herbicide Treatment in La Ribera District, Spain. *Journal of Environmental Management* **2021**, *282*, 111965, https://doi.org/10.1016/J.JENVMAN.2021.111965.
12. Valle, A.L.; Mello, F.C.C.; Alves-Balvedi, R.P.; Rodrigues, L.P.; Goulart, L.R. Glyphosate Detection: Methods, Needs and Challenges. *Environmental Chemistry Letters 2018 17:1* **2018**, *17*, 291–317, https://doi.org/10.1007/S10311-018-0789-5.
13. Chen, H.; Hu, O.; Fan, Y.; Xu, L.; Zhang, L.; Lan, W.; Hu, Y.; Xie, X.; Ma, L.; She, Y.; et al. Fluorescence Paper-Based Sensor for Visual Detection of Carbamate Pesticides in Food Based on CdTe Quantum Dot and Nano ZnTPyP. *Food Chemistry* **2020**, *327*, 127075, https://doi.org/10.1016/J.FOODCHEM.2020.127075.
14. Singh, R.; Kumar, N.; Mehra, R.; Kumar, H.; Singh, V.P. Progress and Challenges in the Detection of Residual Pesticides Using Nanotechnology Based Colorimetric Techniques. *Trends in Environmental Analytical Chemistry* **2020**, *26*, e00086, https://doi.org/10.1016/J.TEAC.2020.E00086.
15. Ullah, N.; Mansha, M.; Khan, I.; Qurashi, A. Nanomaterial-Based Optical Chemical Sensors for the Detection of Heavy Metals in Water: Recent Advances and Challenges. *TrAC Trends in Analytical Chemistry* **2018**, *100*, 155–166, https://doi.org/10.1016/J.TRAC.2018.01.002.
16. Cao, S.; Qi, J.; Lei, F.; Wei, Z.; Lou, S.; Yang, X.; Guo, Y.; Hao, P.; Xie, J.; Tang, B. Reduction-Induced Surface Reconstruction to Fabricate Cobalt Hydroxide/Molybdenum Oxide Hybrid Nanosheets for Promoted Oxygen Evolution Reaction. *Chemical Engineering Journal* **2021**, *413*, 127540, https://doi.org/10.1016/J.CEJ.2020.127540.
17. Onwudiwe, D.C.; Ravele, M.P.; Elemike, E.E. Eco-Friendly Synthesis, Structural Properties and Morphology of Cobalt Hydroxide and Cobalt Oxide Nanoparticles Using Extract of Litchi Chinensis. *Nano-Structures & Nano-Objects* **2020**, *23*, 100470, https://doi.org/10.1016/J.NANOSO.2020.100470.
18. Heineke, D.; Franklin, S.J.; Raymond, K.N. Coordination Chemistry of Glyphosate: Structural and Spectroscopic Characterization of Bis(Glyphosate)Metal(III) Complexes. *Inorganic Chemistry* **1994**, *33*, 2413–2421, https://doi.org/10.1021/ic00089a017.
19. Uskoković, V. Nanotechnologies: What We Do Not Know. *Technology in Society* **2007**, *29*, 43–61, https://doi.org/10.1016/J.TECHSOC.2006.10.005.
20. Madalena, D.A.; Ramos, Ó.L.; Pereira, R.N.; Bourbon, A.I.; Pinheiro, A.C.; Malcata, F.X.; Teixeira, J.A.; Vicente, A.A. In Vitro Digestion and Stability Assessment of β- Lactoglobulin/Riboflavin Nanostructures. *Food Hydrocolloids* **2016**, *58*, 89–97, https://doi.org/10.1016/J.FOODHYD.2016.02.015.
21. Yang, J.; Liu, H.; Martens, W.N.; Frost, R.L. Synthesis and Characterization of Cobalt Hydroxide, Cobalt Oxyhydroxide, and Cobalt Oxide Nanodiscs. *Journal of Physical Chemistry C* **2010**, *114*, 111–119, https://doi.org/10.1021/jp908548f.

22. Tian, L.; Zhu, J.L.; Chen, L.; An, B.; Liu, Q.Q.; Huang, K.L. Synthesis and Characterization of α-Cobalt Hydroxide Nanobelts. *Journal of Nanoparticle Research 2011 13:8* **2011**, *13*, 3483–3488, https://doi.org/10.1007/S11051-011-0269-3.
23. Souza, T.G.F.; Ciminelli, V.S.T.; Mohallem, N.D.S. A Comparison of TEM and DLS Methods to Characterize Size Distribution of Ceramic Nanoparticles. *Journal of Physics: Conference Series* **2016**, *733*, 012039, https://doi.org/10.1088/1742-6596/733/1/012039.
24. Rahbani, J.; Khashab, N.M.; Patra, D.; Al-Ghoul, M. Kinetics and Mechanism of Ionic Intercalation/de-Intercalation during the Formation of α-Cobalt Hydroxide and Its Polymorphic Transition to β-Cobalt Hydroxide: Reaction–Diffusion Framework. *Journal of Materials Chemistry* **2012**, *22*, 16361–16369, https://doi.org/10.1039/C2JM31694C.
25. Li, H.B.; Yu, M.H.; Lu, X.H.; Liu, P.; Liang, Y.; Xiao, J.; Tong, Y.X.; Yang, G.W. Amorphous Cobalt Hydroxide with Superior Pseudocapacitive Performance. *ACS Applied Materials and Interfaces* **2014**, *6*, 745–749, https://doi.org/10.1021/AM404769Z.
26. Zhao, T.; Jiang, H.; Ma, J. Surfactant-Assisted Electrochemical Deposition of α-Cobalt Hydroxide for Supercapacitors. *Journal of Power Sources* **2011**, *196*, 860–864, https://doi.org/10.1016/J.JPOWSOUR.2010.06.042.
27. Li, H.B.; Yu, M.H.; Lu, X.H.; Liu, P.; Liang, Y.; Xiao, J.; Tong, Y.X.; Yang, G.W. Amorphous Cobalt Hydroxide with Superior Pseudocapacitive Performance. *ACS Applied Materials and Interfaces* **2014**, *6*, 745–749, https://doi.org/10.1021/AM404769Z.
28. Österberg, M.; Sipponen, M.H.; Mattos, B.D.; Rojas, O.J. Spherical Lignin Particles: A Review on Their Sustainability and Applications. *Green Chemistry* **2020**, *22*, 2712–2733, https://doi.org/10.1039/D0GC00096E.
29. Zhu, H.; Quan, Z.; Hou, H.; Cai, Y.; Liu, W.; Liu, Y. A Colorimetric Immunoassay Based on Cobalt Hydroxide Nanocages as Oxidase Mimics for Detection of Ochratoxin A. *Analytica Chimica Acta* **2020**, *1132*, 101–109, https://doi.org/10.1016/J.ACA.2020.07.068.
30. Hou, Y.; Kondoh, H.; Shimojo, M.; Kogure, T.; Ohta, T. High-Yield Preparation of Uniform Cobalt Hydroxide and Oxide Nanoplatelets and Their Characterization. *Journal of Physical Chemistry B* **2005**, *109*, 19094–19098, https://doi.org/10.1021/jp0521149.
31. Liu, X.; Yi, R.; Zhang, N.; Shi, R.; Li, X.; Qiu, G. Cobalt Hydroxide Nanosheets and Their Thermal Decomposition to Cobalt Oxide Nanorings. *Chemistry – An Asian Journal* **2008**, *3*, 732–738, https://doi.org/10.1002/ASIA.200700264.
32. Xu, Z.P.; Zeng, H.C. Thermal Evolution of Cobalt Hydroxides: A Comparative Study of Their Various Structural Phases. *Journal of Materials Chemistry* **1998**, *8*, 2499–2506, https://doi.org/10.1039/A804767G.
33. Chang, Y.; Zhang, Z.; Hao, J.; Yang, W.; Tang, J. A Simple Label Free Colorimetric Method for Glyphosate Detection Based on the Inhibition of Peroxidase-like Activity of Cu(II). *Sensors and Actuators B: Chemical* **2016**, *228*, 410–415, https://doi.org/10.1016/J.SNB.2016.01.048.
34. Zheng, J.; Zhang, H.; Qu, J.; Zhu, Q.; Chen, X. Visual Detection of Glyphosate in Environmental Water Samples Using Cysteamine-Stabilized Gold Nanoparticles as Colorimetric Probe. *Analytical Methods* **2013**, *5*, 917–924, https://doi.org/10.1039/C2AY26391B.
35. Xiao, M.; Wang, Z.; Lyu, M.; Luo, B.; Wang, S.; Liu, G.; Cheng, H.M.; Wang, L. Hollow Nanostructures for Photocatalysis: Advantages and Challenges. *Advanced Materials* **2019**, *31*, 1801369, https://doi.org/10.1002/ADMA.201801369.
36. Hansen, L.R.; Roslev, P. Behavioral Responses of Juvenile Daphnia Magna after Exposure to Glyphosate and Glyphosate-Copper Complexes. *Aquatic Toxicology* **2016**, *179*, 36–43, https://doi.org/10.1016/J.AQUATOX.2016.08.010.
37. de Almeida, L.K.S.; Chigome, S.; Torto, N.; Frost, C.L.; Pletschke, B.I. A Novel Colorimetric Sensor Strip for the Detection of Glyphosate in Water. *Sensors and Actuators B: Chemical* **2015**, *206*, 357–363, https://doi.org/10.1016/J.SNB.2014.09.039.
38. Lopes, F.A.; Ferreira, G.R.; Franco, M.R.; Schimitberger, T.; de Faria, L.O.; Bianchi, R.F. A Versatile Radiochromic Dosimeter for Low-Medium Gamma Radiation and Its Application to Food Irradiation. *Journal of Applied Polymer Science* **2018**, *135*, 45729, https://doi.org/10.1002/APP.45729.